RhoA Signaling and Synaptic Damage Occur Within Hours in a Live Pig Model of CNS Injury, Retinal Detachment

Jianfeng Wang,[1] Marco Zarbin,[2] Ilene Sugino,[2] Ian Whitehead,[3] and Ellen Townes-Anderson[1]

[1]Department of Pharmacology, Physiology, and Neuroscience, New Jersey Medical School-Rutgers Biomedical Health Sciences, Rutgers University, Newark, New Jersey, United States
[2]Institute of Ophthalmology and Visual Science, New Jersey Medical School-Rutgers Biomedical Health Sciences, Rutgers University, Newark, New Jersey, United States
[3]Department of Microbiology, Biochemistry, and Medical Genetics, New Jersey Medical School-Rutgers Biomedical Health Sciences, Rutgers University, Newark, New Jersey, United States

Correspondence: Ellen Townes-Anderson, Department of Pharmacology, Physiology, and Neuroscience, New Jersey Medical School-Rutgers Biomedical Health Sciences, 185 South Orange Avenue, Rutgers University, Newark, NJ 07103, USA; andersel@njms.rutgers.edu.

Submitted: February 26, 2016
Accepted: June 9, 2016

Citation: Wang J, Zarbin M, Sugino I, Whitehead I, Townes-Anderson E. RhoA signaling and synaptic damage occur within hours in a live pig model of CNS injury, retinal detachment. *Invest Ophthalmol Vis Sci*. 2016;57:3892–3906. DOI:10.1167/iovs.16-19447

Purpose. The RhoA pathway is activated after retinal injury. However, the time of onset and consequences of activation are unknown in vivo. Based on in vitro studies we focused on a period 2 hours after retinal detachment, in pig, an animal whose retina is holangiotic and contains cones.

Methods. Under anesthesia, retinal detachments were created by subretinal injection of a balanced salt solution. Two hours later, animals were sacrificed and enucleated for GTPase activity assays and quantitative Western blot and confocal microscopy analyses.

Results. RhoA activity with detachment was increased 1.5-fold compared to that in normal eyes or in eyes that had undergone vitrectomy only. Increased phosphorylation of myosin light chain, a RhoA effector, also occurred. By 2 hours, rod cells had retracted their terminals toward their cell bodies, disrupting the photoreceptor-to-bipolar synapse and producing significant numbers of spherules with SV2 immunolabel in the outer nuclear layer of the retina. In eyes with detachment, distant retina that remained attached also showed significant increases in RhoA activity and synaptic disjunction. Increases in RAC1 activity and glial fibrillary acidic protein (GFAP) were not specific for detachment, and sprouting of bipolar dendrites, reported for longer detachments, was not seen. The RhoA kinase inhibitor Y27632 significantly reduced axonal retraction by rod cells.

Conclusions. Activation of the RhoA pathway occurs quickly after injury and promotes synaptic damage that can be controlled by RhoA kinase inhibition. We suggest that retinal detachment joins the list of central nervous system injuries, such as stroke and spinal cord injury, that should be considered for rapid therapeutic intervention.

Keywords: photoreceptor, retinal detachment, RhoA, ROCK, synaptic plasticity

The contribution of RhoA signaling to the inhibition of axonal growth after central nervous system (CNS) injury is well established. Increases in the expression and/or activity of RhoA, a member of the Rho family of GTPases, have been observed in traumatic brain injury and stroke in humans[1,2] and in animal models of spinal cord injury, epilepsy, and Alzheimer's disease.[3–6] Conversely, blocking the RhoA signaling pathway either directly by inhibiting RhoA activation or by inhibiting the downstream target Rho-associated kinase (ROCK) has been shown to promote CNS regeneration after injury both in vitro and in vivo[7,8] and to be neuroprotective for stroke and Parkinson's and Alzheimer's disease.[9–12]

What is not yet clear is how quickly RhoA signaling occurs after injury to the CNS. Most animal models examine RhoA protein, mRNA, or activation days or weeks after the initial insult. However, understanding the timing of the activation of this pathway is critical in order to optimize the approach and timing of therapeutic intervention with RhoA inhibitory drugs. One report showed increased RhoA activation 1.5 hours after spinal cord transection in rat.[4] The result is suggestive of early RhoA activation, but it was not pursued quantitatively. In our view, it is conceivable that increased RhoA activity will add to the list of CNS injury responses that need to be handled within a matter of hours to improve recovery.

Here, we used a well-controlled in vivo model of CNS injury, retinal detachment, to explore the possibility of acute activation of RhoA and some of its downstream targets (Fig. 1) and to correlate biochemical results with structural damage to the retina. Using an in vitro system, we previously determined that RhoA activation plays a role in the retina's injury response to detachment.[13,14] In humans, the response to retinal detachment features synaptic plasticity in the form of retraction and growth of nerve cell processes.[15,16] The earliest structural change is retraction of rod photoreceptor axon terminals toward their cell bodies, resulting in the disjunction of the first synapse in the visual pathway, the synapse between the photoreceptors and the bipolar and horizontal cells.[17–20] Using both isolated amphibian rod cells and cultured porcine retina, we found that inhibiting RhoA and ROCK activation dramatically reduced synaptic disjunction.[14] In the present report, we performed in vivo retinal detachment in pigs, because the pig eye is very similar to the human eye in size,

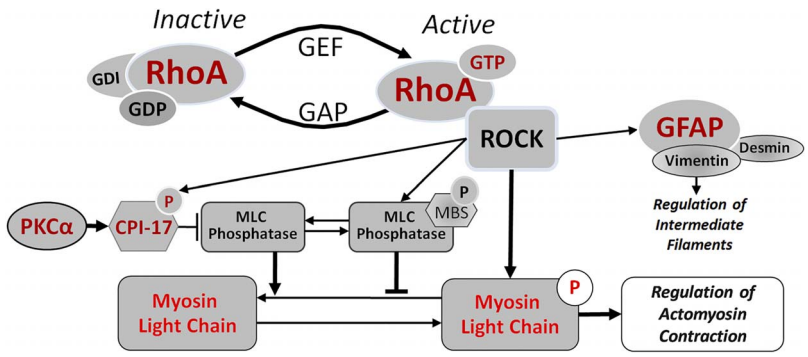

Figure 1. Proposed signaling pathway in retinal detachment leading to rod terminal retraction. RhoA activation leads to phosphorylation of MLC, causing actomyosin contraction, and is responsible in part for axonal retraction. Components of the RhoA signaling pathway (*red*), as well as another Rho protein, RAC1, and myosin IIB, which contains MLC, were examined. MBS, myosin binding subunit; MLC, myosin light chain; PAK, p21-activated kinase; GDI, guanosine nucleotide dissociation inhibitor; GDP, guanosine diphosphate; GEF, guanine nucleotide exchange factor; GTP, guanosine triphosphate; GAP, GTPase activating proteins.

vasculature, and neuronal morphology and contains an area centralis with an increased cone cell density.[21–23] The results may be translatable to human injury. Based on our in vitro studies, we focused on a period 2 hours after the detachment injury.

Although there is variability among individual animals, in all cases, RhoA activation was significantly and specifically elevated by retinal detachment in as little as 2 hours, with concomitant structural damage to the photoreceptor-bipolar synapses. Moreover, changes occurred in both directly injured and distant neural tissue areas. Finally, application of a ROCK inhibitor successfully reduced synaptic damage. The results may stimulate discussion on the need for rapid treatment of CNS and retinal injury.

Materials and Methods

Animals

For in vitro experiments, pig eyes were obtained from a local abattoir through Animal Parts (Scotch Plains, NJ, USA). The male and female Yorkshire pigs, 6 months old, and weighing 60 to 75 kg, were sacrificed mid-day; the eyes were kept on ice and delivered to the laboratory within 2 hours. For in vivo experiments, female Yorkshire pigs, 3 months old, and weighing 30 kg, obtained from Animal Biotech Industries (Danboro, PA, USA), were kept on a 12L:12D cycle for at least 2 days before surgery. They were housed in an AAALAC-accredited pathogen-free facility, two animals to a pen. The animals were subject to overnight fasting and access to water ad libitum before surgery. Experimental procedures and methods of euthanasia were approved by the New Jersey Medical School Institutional Animal Care and Use Committee and adhered to the ARVO Statement for the Use of Animals in Ophthalmic and Vision Research.

In Vitro Retinal Detachment Model

The in vitro retinal detachments were created as previously described[14,24] with modifications. Briefly, after the surrounding orbital tissue was removed, the eyes were washed twice with Dulbecco's modified Eagle's medium (DMEM) containing 4.5 g/L glucose, L-glutamine, and sodium pyruvate (product 10-013-CV; Cellgro, Mediatech, Manassas, VA, USA). The anterior segment and vitreous body were carefully removed, and a few drops of DMEM were added to keep the surface of the neural retina moist. Seven-millimeter buttons of retinal tissue were created using a trephine and detached from the underlying retinal pigment epithelium (RPE) by injecting a few drops of DMEM along the cut edge. The detached neural retinae were gently removed and cultured in commercial medium (Neurobasal-A; product 10888-022; Gibco, Life Technologies, Grand Island, NY, USA) supplemented with 1% GlutaMAX-I (Gibco), 2% B-27 supplement (Gibco), and 100 U/mL of penicillin and 100 μg/mL streptomycin (Gibco) at 37°C. Cultured retinae were snap-frozen with dry ice plus ethanol after 0, 1, or 10 minutes or 2 hours and stored at –80°C for further use. A total of six eyes yielding 30 retinal explants were used.

In vivo Retinal Detachment Model

Animals were sedated with ketamine (20 mg/kg; Mylan Institutional LLC, Galway, Ireland) and xylazine (2.2 mg/kg; Lloyd Lab., Shenandoah, IA, USA) injected intramuscularly and then catheterized and intubated. To maintain anesthesia, the animals were supplied with 0.5% to 2.0% isoflurane in oxygen using a ventilator. Lactated Ringer's solution was infused intravenously at a rate of 8 mL/kg/h. Under anesthesia, pupils were dilated with topical application of 1% cyclopentolate (Cyclogyl; Alcon, Fort Worth, TX, USA) and 2.5% phenylephrine (Paragon Bioteck, Portland, OR, USA). A standard 3-port vitrectomy was carried using 20-g instrumentation. The posterior hyaloid was detached over the area centralis by using active suction, and a core vitrectomy was completed. During and after vitrectomy, the vitreous cavity of the eye was perfused with a mammalian balanced salt solution (BSS; Alcon) containing 2 μg/mL epinephrine (Henry Schein, Dublin, OH, USA). A bent 33-g metal cannula with a 50 to 100-μm tip was used to slowly inject BSS or RhoA kinase inhibitor Y27632 (Selleckchem, Boston, MA, USA) dissolved in BSS subretinally to create retinal detachment (~10–15 mm in diameter) in the inferior nasal quadrant (Fig. 2A). After the detachment was created, the animal was kept under anesthesia for 2 hours and then sacrificed for enucleation. The control eyes received either no surgery or only a vitrectomy (including posterior hyaloid excision) without retinal detachment. Eyes were kept in ice-cold DMEM until opened to collect samples, usually approximately 20 minutes later. Sample collection is diagrammed in Figures 2A and 2B. Areas of some depigmentation were present in the area centralis and peripapillary retinae of three animals before surgery (Fig. 2C); occasionally some RPE

Investigative Ophthalmology & Visual Science

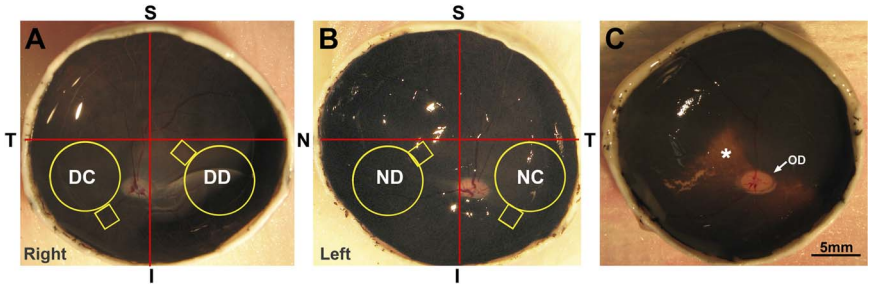

Figure 2. Location of retinal detachment in vivo and sample collection. (**A**, **B**) Retinal detachments were created in the inferior nasal quadrant after vitrectomy. Samples from the trephined (*round*) areas were subjected to biochemical analysis, whereas the square areas were used for morphological analysis. (**C**) Depigmentation was observed in some areas (*) in animals used in this study. DD, detached area; DC, attached, control area; ND, normal eye, area corresponding to DD; NC, normal eye, area corresponding to DC; T, Temporal; N, Nasal; S, Superior; I, Inferior; OD, optic disc.

was debrided during creation of the detachment. Once the eyes were harvested, the neural retinal tissues were collected as described above and kept at −80°C for biochemical analysis or were fixed in 4% paraformaldehyde (EMS, Hatfield, PA, USA) for morphological analysis. A total of 19 animals and 38 eyes were used.

Western Blotting

To prepare retinal samples for Western blotting, trephined retinae (7-mm diameter buttons) were lysed, homogenized in 1× radioimmunoprecipitation assay buffer (EMD Millipore, Billerica, MA, USA) containing 1× protease inhibitor (Roche, New York, NY, USA), 2 mM Na_3VO_4, and 10 mM NaF with ceria stabilized zirconium oxide beads (0.5 mm in diameter, ZrOB05; Next Advance, Averill Park, NY, USA), and centrifuged at 15,000*g* for 10 minutes at 4°C. Protein concentrations were determined using a protein assay kit (Quick Start Bradford protein kit; Bio-Rad, Hercules, CA, USA). The samples were then dispersed in an equal volume of 2× SDS loading buffer (Bio-Rad) containing 10% 2-mercaptoethanol, and boiled for 5 minutes; assayed by electrophoresis, using 10% or 8% to 16% precast polyacrylamide gels (Bio-Rad); transferred to a nitrocellulose membrane (0.2 μm; Bio-Rad), and analyzed by Western blotting. The following antibodies were used: RhoA rabbit monoclonal antibody (mAb), phosphorylated myosin light chain 2 (pMLC [Ser-19]) mouse mAb, myosin light chain 2 (MLC) rabbit mAb and protein kinase C alpha (PKCα) rabbit polyclonal antibody (pAb) (all from Cell Signaling, Boston, MA, USA), di-phosphorylated MLC 2 (di-pMLC [Thr-18/Ser-19]) rabbit mAb (Thermo Scientific, Rockford, IL, USA), RAC1 mouse mAb (Becton Dickinson, Franklin Lakes, NJ, USA), p-CPI-17 rabbit pAb (Santa Cruz Biotechnology, Dallas, TX, USA), synaptic vesicle protein 2 (SV2) and myosin IIB mouse mAb (Developmental Studies Hybridoma Bank, Iowa City, IA, USA), and glial fibrillary acidic protein (GFAP) rabbit pAb (Dako, Carpinteria, CA, USA). For an internal control, glyceraldehyde-3-phosphate dehydrogenase rabbit (GAPDH) pAb (Santa Cruz Biotechnology) was blotted in the same membrane. The membranes were visualized using secondary goat anti-mouse or rabbit immunoglobulin G (IgG) antibody conjugated to horseradish peroxidase (Jackson ImmunoResearch Laboratories, West Grove, PA, USA). Luminata Classico or Forte Western horseradish peroxidase substrates (EMD Millipore) were used to visualize the immune complexes. The density of a specific band was determined using ImageJ software (version 1.45s; US National Institutes of Health, Bethesda, MD, USA, http://imagej.nih.gov/ij/, available in the public domain).

Immunohistochemistry

Specimens, fixed in 4% paraformaldehyde in 0.125 M phosphate buffer (PB [pH 7.4]), were immersed in 30% sucrose overnight at 4°C, embedded, frozen in OCT compound (Sakura Finetek, Torrance, CA, USA), and cut into 15-μm-thick sections by using a cryostat, as described previously.[24] In some cases, the specimens were snap frozen in OCT compound with dry ice plus ethanol (95%) and cut into 20-μm-thick sections, followed by 10-minute fixation in ethanol (95%). Sections were immunolabeled for RhoA, RAC1, PKCα, GFAP, SV2, di-pMLC, and myosin IIB by using the antibodies listed above.

For fluorescence immunolabeling, the sections were labeled with secondary antibodies conjugated to Alexa Fluor 488, 546, or 647 (Life Technologies, Norwalk, CT, USA), followed by staining with 1 μg/mL propidium iodide (PI; Sigma-Aldrich, St. Louis, MO, USA) or TO-PRO3 (1:500 dilution; Life Technologies) to stain nuclei. Sections were covered with Fluoromount-G medium (SouthernBiotech, Birmingham, AL, USA) and preserved under coverslips sealed with nail polish. Sections were examined using confocal microscopy (model LSM510; Carl Zeiss Microscopy, Jena, Germany) by scanning 1.5-μm optically thick sections with a 40× water immersion objective or 1.0-μm optically thick sections with a 63× oil immersion objective.

For all immunohistochemistry, control sections were processed simultaneously with experimental sections but without primary antibodies.

TUNEL Staining

TUNEL staining was performed according to the manufacturer's instructions, using a TACS 2 TdT-Fluor in situ apoptosis detection kit (Trevigen, Gaithersburg, MD, USA).

RhoA and RAC1 Activation Assay

Rhotekin-RBD (rho binding domain) beads (Cytoskeleton, Denver, CO, USA) were used to precipitate activated GTP-bound RhoA from retinal samples. To precipitate active GTP-bound RAC1, the p21 binding domain of Pak3 (PAK-GST-PBD)[25] expressed in *Escherichia coli* as glutathione *S*-transferase (GST) fusion proteins and immobilized by binding to glutathione-Sepharose 4B beads (Thermo Scientific) was used. Retinal samples were lysed as described above (in *Western Blotting*) and immediately added to 40 μg of Rhotekin-RBD beads or 60 μg of PAK-GST-PBD beads. The mixture was incubated for 1 hour at 4°C, then centrifuged for 2 minutes at 5000 rpm at 4°C, washed once with excess lysis buffer and twice with phosphate buffer saline (PBS), resuspended in 40

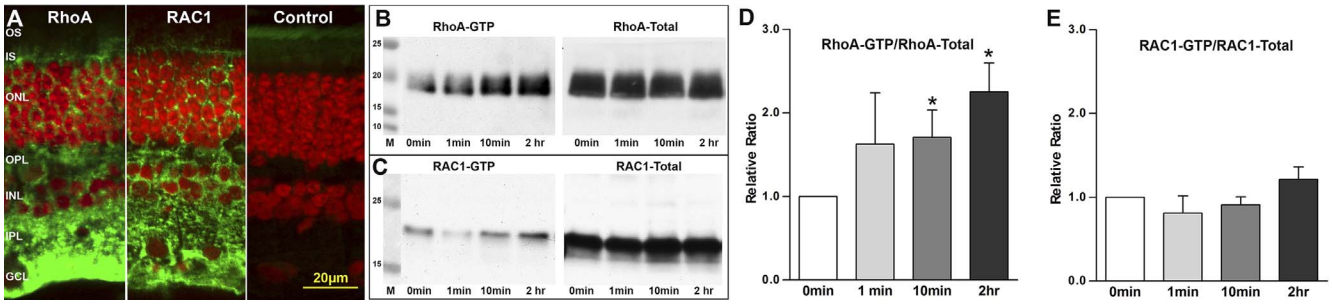

Figure 3. RhoA and RAC1 activation in vitro. (**A**) RhoA and RAC1 proteins (*green*) are found throughout the normal pig neural retina. Control labeling without primary antibody showed little background except for some nonspecific fluorescence in the OS. *red*, nuclei stained with propidium iodide. (**B**, **C**) Typical Western blots for total and activated Rho proteins in retinal explants maintained in vitro for varying times. (**D**, **E**) RhoA or RAC1 activity presented as the RhoA-GTP-to-RhoA-Total or Rac1-GTP-to-Rac1-Total ratio and normalized to 1 at time 0. RhoA was activated 1 minute after detachment and was significantly up-regulated by 71% and 125% at 10 minutes and 2 hours, respectively ($n = 19$ retinal explants; five pig eyes; $^*P < 0.01$). RAC1 activity at 2 hours was only 22% higher than that at the 0 time point ($n = 12$ retinal explants; three pig eyes; $P > 0.05$).

μL of 2× Laemmli loading buffer (Bio-Rad), boiled for 3 minutes, and stored at −20°C. RhoA and RAC1 activation assay samples and total retinal protein were analyzed by standard Western blot techniques.

Quantification of Axonal Retraction

All data were collected by researchers blind to the sample identifications. Images of retinal optical sections 1 μm thick were obtained with a laser scanning confocal microscope as described above. Brightness and contrast were set to obtain unsaturated images. Laser power and scanning rate were unchanged throughout a single experiment. Enhancements in brightness and contrast were performed (Photoshop 7.0 software; Adobe, Mountain View, CA, USA) only for presentation purposes. SV2 immunolabeling was analyzed as described previously with some minor modifications.[14] Briefly, a binary mask was created for each image, and the pixels in the outer nuclear layers (ONL) were counted using ImageJ software (NIH). The measurements are reported as pixels per micrometer of the ONL length. In addition, 1 or 2 researchers counted the number of retracted axon terminals manually. Any spot (>1 × 1 μm) with SV2 staining observed in the ONL and at least one cell layer away from the outer plexiform layer (OPL) was counted as one retraction. The counting was reported as number of axonal retractions per 100-μm length of ONL. Data were collected from two to four sections per specimen, examining at least three different areas of each section.

Statistical Analysis

All data were tested with a paired Student's *t* test. The paired *t* test was based on the experimental design. For in vitro experiments, explants from the same eye maintained in culture for differing time points were compared to the control (0 time point). For in vivo experiments, data from the same region of right and left eyes of the same animal or from detached and attached regions of the same retina were paired. For Western blots, the fixed normalization point technique was used; control data were set at 1.[26]

The use of the paired *t* test assumed linearity of the data and a normal distribution of the paired differences. For data from examination of sections, no normalization was done. Statistical analysis was performed with Sigma Plot (version 11; Chicago, IL, USA) or Prism version 5.0 software (GraphPad, La Jolla, CA, USA). The graphics data are expressed as mean ± standard deviation (SD). Statistical significance was set at a *P* value of <0.05.

Results

Increase in RhoA Activity but not in RAC1 Activity In Vitro

To set parameters for biochemical analyses and confirm and expand previous results, we began with an examination of Rho GTPases in the cultured pig retina. Immunofluorescence analysis showed that RhoA expression is found throughout the normal pig retina (Fig. 3A), consistent with our previous findings using two different anti-RhoA antibodies.[14] Our previous study of the detached porcine retina also demonstrated that RhoA activity increased immediately after detachment, returned to normal (a level equivalent to undetached retina) after 2 hours, and then dropped further to below normal after 24 hours.[14] In those experiments, however, the in vitro system contained 10% fetal bovine serum. To limit the possible modulation of RhoA activity by serum components such as lysophosphatidic acid,[27] which is a RhoA activator and can cause neuritic retraction in cultured neuronal cells[28] and photoreceptors,[13] we used a serum-free medium.[29] The RhoA activity was expressed as the GTP-bound RhoA (RhoA-GTP)-to-total RhoA (RhoA-Total) ratio and normalized using 0 minute as 1. At 1 minute after detachment, the RhoA activity was 163% increased compared to that in normal samples (Fig. 3B, 3D), which is similar to what we found when using fortified medium containing serum.[14] However, RhoA activities were further increased to 171% ($P < 0.05$) and 225% ($P < 0.05$) at 10 minutes and 2 hours, respectively, after retinal detachment and culture (Figs. 3B, 3D). Thus RhoA activation in detached retina is not dependent on the presence of serum in our in vitro system. In addition, increases in activity were higher and more prolonged without serum.

RAC1, another Rho GTPase involved in shaping neuronal morphology and observed in photoreceptors, bipolar cells, and ganglion cells in chick retinae at P1,[30] was also found throughout the pig retinae (Fig. 3A). RAC1 had a distribution pattern very similar to that of RhoA. In contrast to RhoA, however, it can promote neuritic outgrowth.[31] In chick retinal neurons, for instance, overexpression of RAC1 induces enhanced neuritogenesis and neuritic branching,[32] whereas attenuation of RAC1 activity may cause disassembly of actin filaments, leading to neurite retraction.[33] To determine

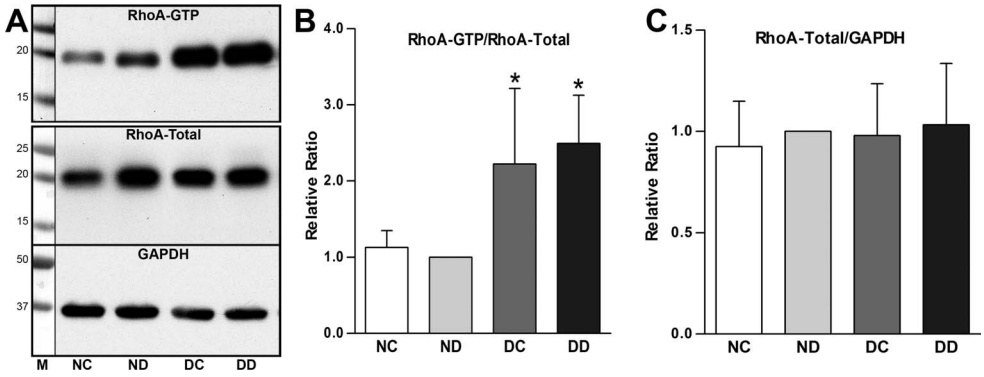

Figure 4. RhoA activation 2 hours after retinal detachment in vivo. (**A**) Typical Western blots of activated and total RhoA (GAPDH, loading control for total RhoA). (**B**) RhoA activity was significantly increased by 149% in detached retina in the operated eye (DD) compared to that in the corresponding area in the control, unoperated eye (ND). RhoA activity in the attached area of the operated eye (DC) was also significantly elevated by 122%. There were no significant differences between DD and DC (*$P < 0.05$; $n = 16$ retinal samples; four pigs). (**C**) Total RhoA levels normalized by GAPDH were similar in all areas of both the operated and the normal, control eye. (Value in ND was normalized to 1.)

whether RAC1 signaling was inhibited or activated after retinal detachment, retinal RAC1 activity was also examined. Similar to results of the RhoA analysis, the active GTP-bound RAC1 (RAC1-GTP)-to-total RAC1 (RAC1-Total) ratios in retinal explants at different time points (0, 1, and 10 minutes and 2 hours) after detachment were compared. RAC1 activity was transiently decreased at 1 minute after detachment and then recovered to a level slightly above (22%; $P > 0.05$) control level (time t = 0) (Figs. 3C, 3E) after 2 hours. There were no significant changes in RhoA or RAC1 protein levels at the different time points (Figs. 3B, 3C, right panels).

Activation of RhoA Signaling In Vivo

RhoA activity in the eye with the detachment was compared to the opposite eye, which received no surgery. The biochemical assay results showed that 2 hours after detachment, RhoA activity in the detached retina of the right eye (DD) was significantly higher (249%; $P < 0.05$) than that in the corresponding area of the left, control eye (ND) (Fig. 4). The RhoA protein, in the nondetached area in the right eye (DC) was also significantly increased (222%; $P < 0.05$) compared to that in the ND. In fact, there were no significant differences in RhoA activity between DD and DC, indicating that activation of RhoA signaling may propagate throughout the whole retina after retinal detachment.

The left, control eye showed no elevation of RhoA activity in any area. The RhoA activity in NC, the area corresponding to DC in the right eye, was similar (106%) to activity in ND (100%). Finally, there were no significant differences in total RhoA protein, which was normalized with the housekeeping protein GAPDH, among the DD, ND, DC, and NC specimens (Fig. 4). Thus, changes in activity appear to be due to the activation of a stable RhoA pool.

There was variability in RhoA activity among animals. Of the 4 animals, 2 showed more than a 2-fold increase in RhoA activity after 2 hours of retinal detachment, whereas the other 2 animals showed an approximate increase of only 40%. Although these data indicate that the extent of the retinal response to traumatic injury may be different between individuals, all animals demonstrated the same trend, RhoA is activated after retinal detachment. In addition, although the eyes used for in vitro experiments came from older animals at approximately 2 hours after death, the results were consistent with the in vivo data from younger animals. Both eyes showed a significant increase in RhoA activity after a 2-hour detachment.

Increase of RAC1 Activity In Vivo

Unlike the in vitro RAC1 activity, which did not change significantly after 2 hours of retinal detachment, the RAC1 activity in the detached retina (DD) of the live pig was observed to have a significant 62% increase ($P < 0.05$) compared to that in ND (Fig. 5) after 2 hours. In the neighboring nondetached retina (DC), there was no significant change in RAC1 activity, indicating the RAC1 signaling may not propagate in 2 hours as RhoA does after retinal detachment in vivo. Also, the extent of the change of RAC1 activity in the detached area was much less than RhoA, 62% versus 122%, suggesting that RhoA signaling may be more responsive than RAC1 signaling to retinal detachment. However, we cannot rule out the possibility that the RhoA assay was more sensitive. Total RAC1 protein remained unchanged at 2 hours, and there were no significant differences in RAC1 activity between DD and DC or between NC and ND (Fig. 5).

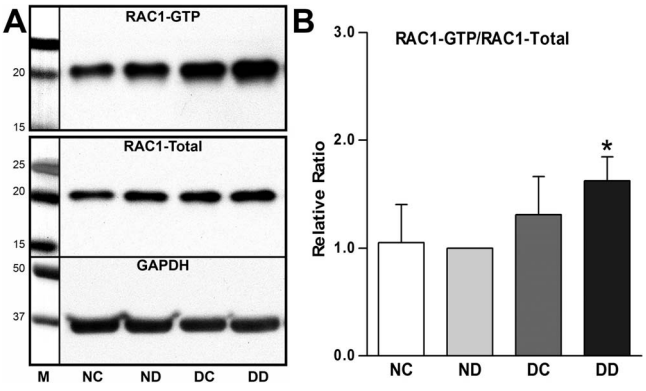

Figure 5. RAC1 activation 2 hours after retinal detachment in vivo. (**A**) Typical Western blot of activated and total RAC1 (GAPDH, loading control for total RAC1). (**B**) RAC1 activity was increased in DD (eye with detachment, detached area) and DC (eye with detachment, attached, control area) by 62% and 31%, respectively. Only the increase in the detached retina (DD) was significant (*$P < 0.05$; $n = 16$ retinal samples; four pigs). Total RAC1 levels were similar in all areas of both the operated and the normal, control eye.

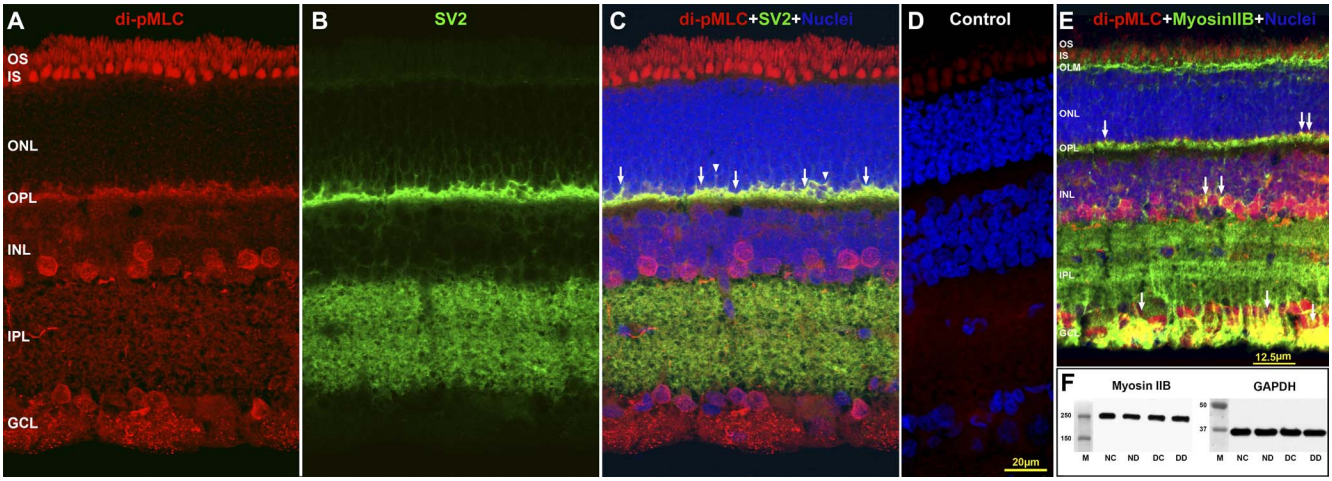

FIGURE 6. Distribution of di-phosphorylated myosin light chain 2 (di-pMLC) and myosin IIB. Optical sections of 1 μm from the attached retina of the operated eye (DC). (**A–C**) Labeling for di-pMLC is present in the GCL, INL, OPL, and photoreceptors IS and OS. Double-staining with SV2 antibody shows colocalization of di-pMLC and SV2 in the OPL ([**C**] *arrows*). The section also showed some axonal retraction (*arrowheads*) by photoreceptors into the ONL. (**D**) Control section shows little background labeling. (**E**) Myosin IIB (*green*) is distributed throughout the neural retina with stronger expression levels in the GCL, OPL, and OLM. *Arrows* indicate areas of colocalization (*yellow*) of myosin IIB (*green*) and di-pMLC (*red*) in the GCL, INL, and OPL. Nuclei were stained with TO-PRO3 (*blue*). (**F**) Western blot analysis from two animals suggested that expression of myosin IIB did not change in the detached retina compared to that in other retinal regions after 2 hours.

Phosphorylation of Myosin Light Chain 2 and Expression of PKCα In Vivo

Myosin is made up of heavy and light chains. Myosin light chain 2 (MLC) can be mono-phosphorylated at Ser-19 or di-phosphorylated at Thr-18 and Ser-19 by the obligate RhoA effector ROCK[34] or by myosin light chain kinase (MLCK)[35] (Fig. 1). Phosphorylation of MLC facilitates activation of the ATPase activity of myosin II, which is critical for actomyosin contraction in nonmuscle cells.[34] For example, myosin II activity is required for severing-induced axon retraction in dorsal root ganglion cells in vitro.[35]

Immunofluorescent labeling for di-pMLC showed that it is present in some cells in the ganglion cell layer (GCL) and inner nuclear layer (INL), as well as in the OPL, where photoreceptors and bipolar cells are connected (Fig. 6A). There was also strong labeling for di-pMLC observed in the outer segment (OS) and inner segment (IS) layers. Double staining with anti-SV2 antibody showed that di-pMLC and SV2 colocalized in the OPL (Figs. 6A–C, arrows). Control tissue showed only very weak fluorescence in these areas (Fig. 6D).

Myosin IIB, one of the vertebrate isoforms of myosin II, has been observed in the inner plexiform layer (IPL), INL, and OPL of adult fish retina and in the outer limiting membrane (OLM) of adult albino trout retina.[36] In the present study, we found myosin IIB label distributed from the inner to the outer retina and especially high at the OLM and in the OPL and inner retina (Fig. 6E). Based on confocal images, we observed myosin IIB and di-pMLC to colocalize only in the GCL, INL, and OPL (Fig. 6E, arrows). It is possible that not all myosin IIB has phosphorylated light chains; furthermore, there may be other myosins in the retina that account for the presence of pMLC in areas where there is no colocalization with myosin IIB.

Western blot analysis of myosin IIB revealed a single band approximately 250 kDa (Fig. 6F), which is in accordance with published results.[36] Densitometric analysis of Western blots from two animals suggested that there was no significant change in myosin llB after retinal detachment (Fig. 6F).

To determine the amount of phosphorylation of MLC before and after retinal detachment, three different antibodies were used for Western blot analysis: antibodies for pMLC (S19), di-pMLC (T18/S19), and MLC. Two dominant bands of approximately 25 kDa and 50 kDa were observed with all three antibodies (Figs. 7A–C). The 25-kDa band was somewhat larger than the predicted mass of MLC, which may be due to factors that affect the migration of proteins on SDS-PAGE, such as post-translational modification. The 50-kDa band could be the dimer of that 25-kDa band. Because the 50-kDa band was detected by using Western blot by another group[37] and was predominant, it was used for densitometric analysis. Quantitative analysis showed that the pMLC-to-MLC ratio was increased in the detached area (DD) by 147% ($P < 0.05\%$) and in the nondetached area (DC) by 47% (although this was not statistically significant), compared to the control (ND) (Fig. 7D). MLC protein levels did not change during this time. Thus, immunolabeling and Western blot analysis demonstrated the presence of MLC in retina and increased phosphorylation after retinal detachment in the areas directly injured and a trend toward increased phosphorylation in distant retina.

In smooth muscle, phosphorylation of MLC can be mediated either by PKCα and phosphorylation of the protein kinase C-potentiated phosphatase inhibitor of 17 kDa (pCPI-17), observed as a dimer, a 34-kDa band on Western blot, or the RhoA/ROCK signaling pathway depending on the cross-talk between these two signaling pathways.[38] PKCα is also a well-known marker for rod bipolar cells in the INL.[18] Western blot analysis of PKCα and pCPI-17 revealed bands at 80 and 34 kDa, respectively, which increased but not significantly, in both DD and DC compared to ND (Figs. 7E–G). These results suggest that if pCPI-17 contributes to the increased accumulation of pMLC by inhibiting phosphatase, the effect is limited.

Changes in GFAP Protein Levels

GFAP is expressed mainly in Müller cells, which are specialized radial glial cells spanning the thickness of the neural retina from the vitreous surface (i.e., inner limiting membrane [ILM]) to the OLM (i.e., the level of the photoreceptor IS).[39] The activation of glial cells, which is characterized by an up-regulation of immunoreactivity for the intermediate filament constituents vimentin and GFAP, begins within minutes of detachment and proceeds during the first few hours and days

Investigative Ophthalmology & Visual Science

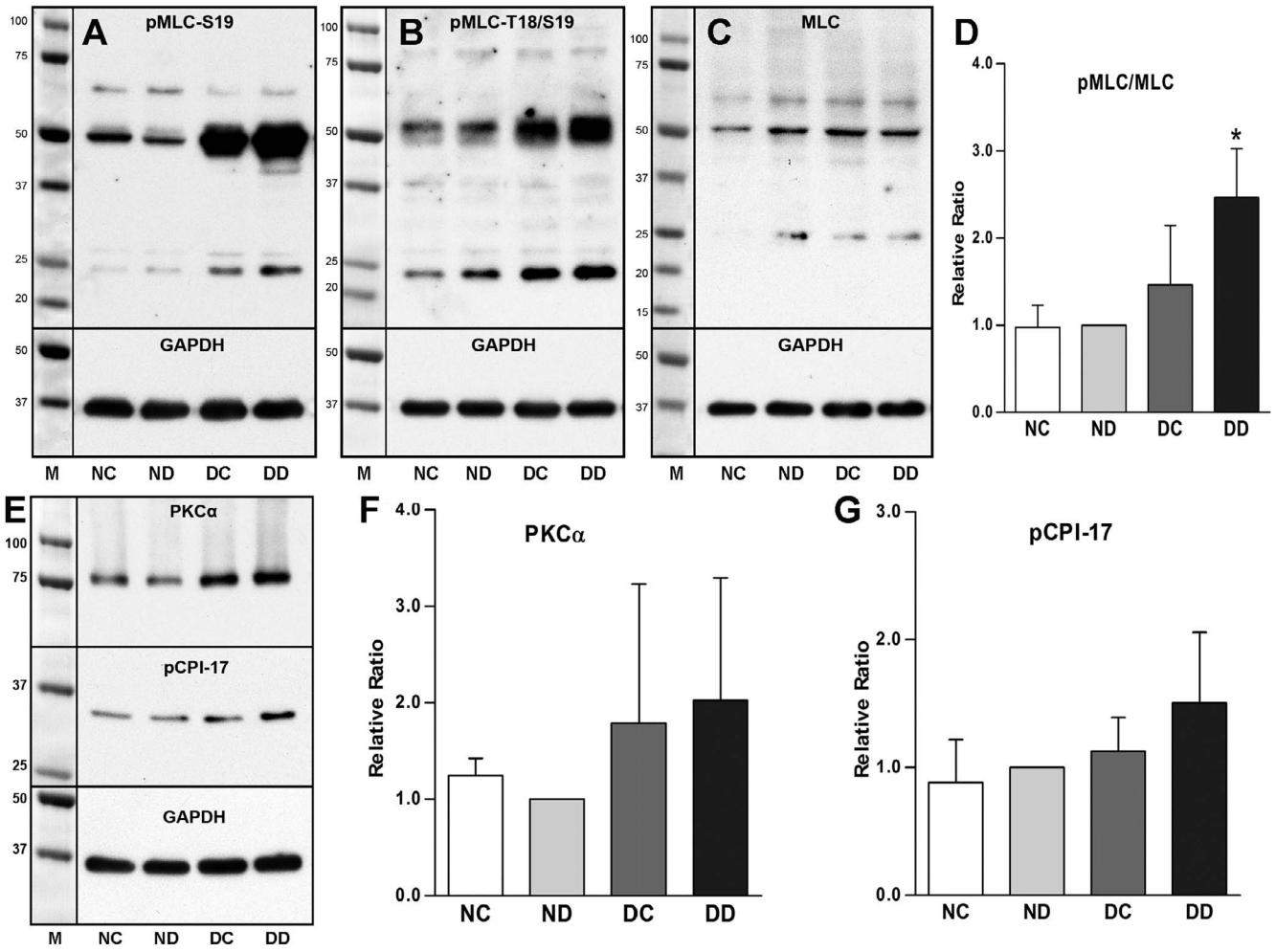

Figure 7. Phosphorylated MLC, PKCα, and pCPI-17 2 hours after retinal detachment in vivo. (**A**–**C**) Antibodies against single- and di-phosphorylated MLC both produced bands of approximately 25 kDa and 50 kDa, in Western blots. We considered the 25-kDa band to be post-translationally modified MLC and the 50-kDa band to be a dimer of the 25-kDa band. (**D**) The stronger, more consistent 50-kDa band of the pMLC antibody (S19) was used to calculate phosphorylation levels of MLC. The pMLC was increased 147% in DD (*$P < 0.05$) and 47% in DC ($P > 0.05$; $n =$ 16 retinal samples; four pigs). (**E**) Typical Western blot for PKCα and pCPI-17. (**F**, **G**) PKCα was up-regulated in DD areas and DC areas of the operated eye. pCPI-17, an inhibitory phosphoprotein for myosin phosphatase, was also slightly elevated in DD. These increases however were not significant ($n = 16$ retinal samples, four pigs).

after retinal detachment.[19,40] Retinal GFAP levels are thought to be sensitive to increased RhoA activity, as levels can be reduced by ROCK inhibitors in optic nerve injury.[41] We also found that immunoreactivity for GFAP was dramatically increased after 2 hours of detachment in vivo (Figs. 8A, 8B). In the control eye, GFAP was expressed mainly in the Müller cell endfeet in the GCL and ILM, whereas it was highly expressed in both the endfeet and the glial soma throughout, from ILM to OLM after detachment (DD). The distribution pattern of GFAP in DC was similar to that observed in DD. Quantification of GFAP by Western blot analysis showed that the total amount of GFAP was increased by 150% ($P < 0.01$) in DD and 94% in DC ($P = 0.08$) (Figs. 8C, 8D). The increase in the distribution of molecular weights suggests that lower-weight isoforms were also expressed after detachment.

Vitrectomy Does Not Affect RhoA Activation in Retina

In order to verify that the activation of Rho signaling was due to detachment and not simply due to the surgery, three additional animals were examined along with surgical controls. The right eyes underwent vitrectomy and retinal detachment, whereas the left eyes received vitrectomy alone and served as the controls. The RhoA activity assay showed that the RhoA activity in detached (DD) and attached (DC) areas in the right eyes was 179% ($P < 0.05$) and 101% ($P < 0.01$), respectively, greater than that of the vitrectomy-only control (VD) eye in the corresponding areas (Figs. 9A, 9B). The percentage increase was similar to that found when RhoA activity in untouched eyes was compared to eyes with a detachment (Figs. 4B, 9B). The phosphorylation of MLC was also increased in DC and DD compared to that in vitrectomy alone in all animals; the range of increases was broad, specifically, pMLC increased by 17%, 68%, and 111% ($P = 0.07$) for the detached area compared to the vitrectomized eyes (Figs. 9C, 9D). Thus, higher RhoA activity and potentially higher activity in the RhoA pathway in the right eye were due to the retinal detachment and not to vitrectomy.

In contrast, RAC1 activity was low and showed no differences among all the experimental groups (Figs. 9C, 9E). Western blot analysis of GFAP in these same animals showed that there was also no significant change in the expression level of GFAP among VC, VD, DC, and DD (Figs. 9A, 9F). The

Investigative Ophthalmology & Visual Science

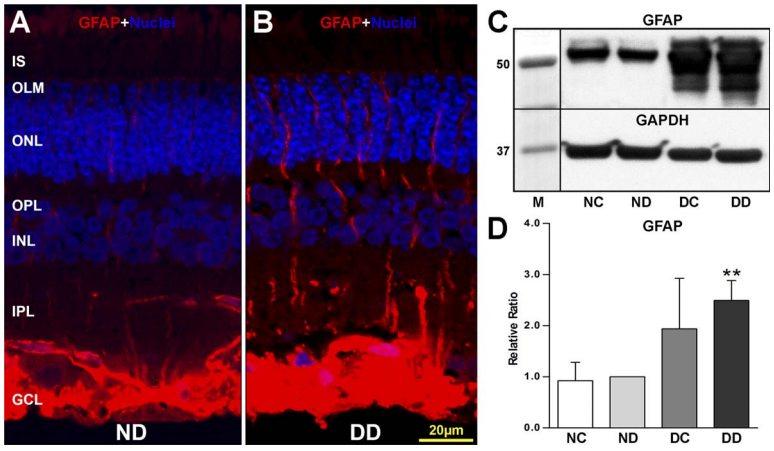

Figure 8. GFAP 2 hours after detachment in vivo. (**A**, **B**) Immunolabeling showed a robust increase of GFAP (*red*) expression in Müller cells in detached (DD) compared to normal, control (ND) retina (nuclei stained *blue* with PI). (**C, D**) GFAP levels in DD and attached (DC) retinal areas were elevated 150% (**$P < 0.01$) and 94% ($P = 0.08$), respectively, compared to those in ND ($n = 16$ retinal samples, four pigs).

levels of GFAP were relatively high in both eyes (compare with Fig. 8C), indicating that Müller/glial cells after vitrectomy may be activated through signaling pathways other than RhoA signaling.

Axonal Retraction by Photoreceptors After Retinal Detachment

If RhoA activity is up-regulated within 2 hours in a retina with detachment, does structural synaptic plasticity also begin early? Normally, the distribution of SV2 in porcine retina is strictly limited to the OPL and IPL, where the synapses between photoreceptors and bipolar and horizontal cells or between bipolar cells and amacrine and ganglion cells are present.[14,42] Under certain conditions, such as retinal detachment, the connection between photoreceptor and bipolar cells may be broken, and the axonal terminals retract toward their cell bodies as indicated by the presence of SV2-labeled spots in the ONL, where the cell bodies of photoreceptors are located.[20,42]

For quantification of axonal retraction, a bright green spot in focus in optical sections of the ONL was counted as one retraction (Figs. 10A–C). The analysis showed that the number of retractions per 100 μm of retina was 4.6 and 4.4 in DD and DC, respectively, which was 171% ($P < 0.05$) and 160% ($P < 0.01$) higher than that in VD (1.7 spots/100 μm retina) (data not shown). If the eye is not operated on and is fixed immediately after enucleation, almost no spots are observed as previously described[14] (Fig. 11E).

When the contrast between axonal terminals and background staining was high, it was easy to tell which spot was a retracted terminal, and the manual counting method worked well. However, if the contrast was poor, that is, background staining was high, it became more difficult to determine the retracted terminals in the ONL, and the results obtained with a manual count became more subjective. In order to reduce the subjective determination of terminal retraction, a binary mask was created for each single-channel SV2 immunolabeled image, and the total area of all the pixels within the ONL was measured using ImageJ (Figs. 10D, 10E). Using this method, SV2 immunolabel in the ONL in DD and DC yielded 30.3 pixels/μm of retina and 26.5 pixels/μm of retina, respectively, which were 187% ($P < 0.05$) and 151% ($P < 0.01$), respectively, greater than that observed in the control group VD (10.5 pixels/μm retina) (Fig. 10F). Thus, two separate approaches demonstrated significant changes in synaptic retraction.

Notably, synaptic retraction increased not only in detached retina but also in the undetached areas of the right eye, corresponding to the observation that RhoA signaling spreads to undetached retina in the eye with a detachment. Furthermore, there were no significant differences between detached and undetached areas.

Animals with depigmentation (Fig. 2C) had a pattern of changes in RhoA activity and axonal retraction similar to those in animals without retinal depigmentation. The individual data did not show a correlation between depigmentation and RhoA activity or synaptic retraction.

Normally, the dendritic processes of rod bipolar cells enter the OPL neuropil to reach the rod spherules but never extend into the ONL. It has been shown in the cat retinal detachment model that PKCα-positive processes of rod bipolar cells start to pass the layer of rod terminals and enter the ONL 1 day after retinal detachment; the neurite outgrowth from rod bipolar cells continues to be observed at 3 and 28 days after retinal detachment, which may be a response to retraction of their presynaptic targets, the photoreceptor synaptic terminals.[18,20] In this study, we did not observe labeled processes of rod bipolar cells in the ONL, even though the axonal retraction of photoreceptors was clearly present 2 hours after retinal detachment (Figs. 10B, 10C).

ROCK Inhibitor Y27632 Reduces Photoreceptor Axonal Retraction

Our results establish that rapid structural changes occur in the retina following retinal detachment. Can they be prevented? Our previous in vitro studies showed that 1, 10, or 100 μM Y27632, a ROCK 1 and 2 inhibitor,[43,44] significantly reduced photoreceptor axon retraction following retinal detachment.[14] In order to determine whether inhibition of ROCK can prevent axonal retraction in detached retina in vivo, BSS was used to create a retinal detachment in one eye as control, and 100 μM, 1 mM, or 10 mM Y27632 dissolved in BSS was used to create a retinal detachment in the other eye. The number of SV2-labeled pixels in the different retinal areas (BC and BD, attached and detached areas, respectively, in the eye using BSS for detachment; YC and YD, attached and detached areas, respectively, in the eye using Y27632 for detachment) was compared (Figs. 11A–D). In retinae treated with 100 μM Y27632, the SV2-labeled pixels in YD was 81.2% of that in BD, indicating a reduction of 19.8% in axonal retraction induced by retinal detachment; however, this reduction was not significant.

Investigative Ophthalmology & Visual Science

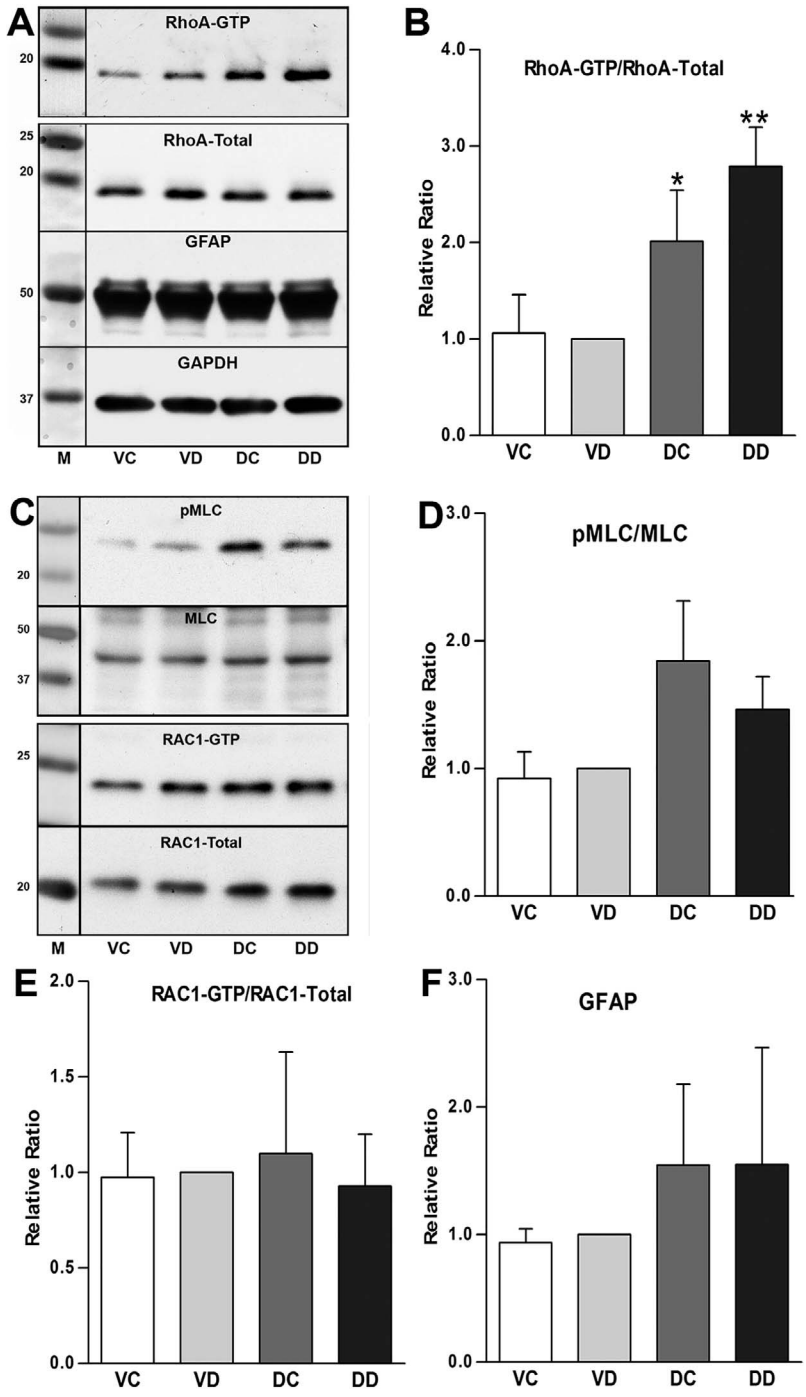

Figure 9. RhoA, pMLC, RAC1, and GFAP 2 hours after detachment compared to vitrectomy alone in vivo. To control for possible effects of ocular surgery, RhoA activity in eyes undergoing vitrectomy was compared with that in eyes with a retinal detachment. (**A**) Typical Western blots of activated and total RhoA and GFAP. (**B**) RhoA activities in detached (DD) and attached (DC) areas of the operated eye were elevated 179% and 101%, respectively, compared to that in retina in eyes that had undergone vitrectomy only (compared to VD), indicating detachment caused a significant elevation in RhoA activity ($^{*}P < 0.05$; $^{**}P < 0.01$; $n = 12$ retinal samples; three pigs). (**C**) Typical Western blots of pMLC and MLC and activated and total RAC1. (**D**) Levels of pMLC were higher in DC and DD than in VD, but the changes in pMLC were not significant in three animals. (**E**) There were no significant differences in RAC1 activity among all groups ($n = 12$ retinal samples, three pigs). (**F**) There were no differences in GFAP levels among all groups ($n = 12$ retinal samples, three pigs).

When the Y27632 dose was increased to 1 mM and 10 mM, the number of SV2-labeled pixels in YD was significantly reduced to 63.3% ($P = 0.02$) and 61.3% ($P = 0.004$), respectively, of that in BD (Figs. 11F, 11G). In the 10 mM Y27632-treated group, the number of SV2-labeled pixels in YC was also significantly reduced to 75.9% ($P = 0.02$) of that in BD (Fig. 11G). Thus, the highest dose of Y27632 was capable of reducing axonal retraction in both attached and detached areas.

In the control groups for 1 mM and 10 mM Y27632, the number of SV2-labeled pixels in the attached area (BC) was not significantly different from that in BD (Figs. 11F, 11G). This is consistent with our previous data which suggested that axonal

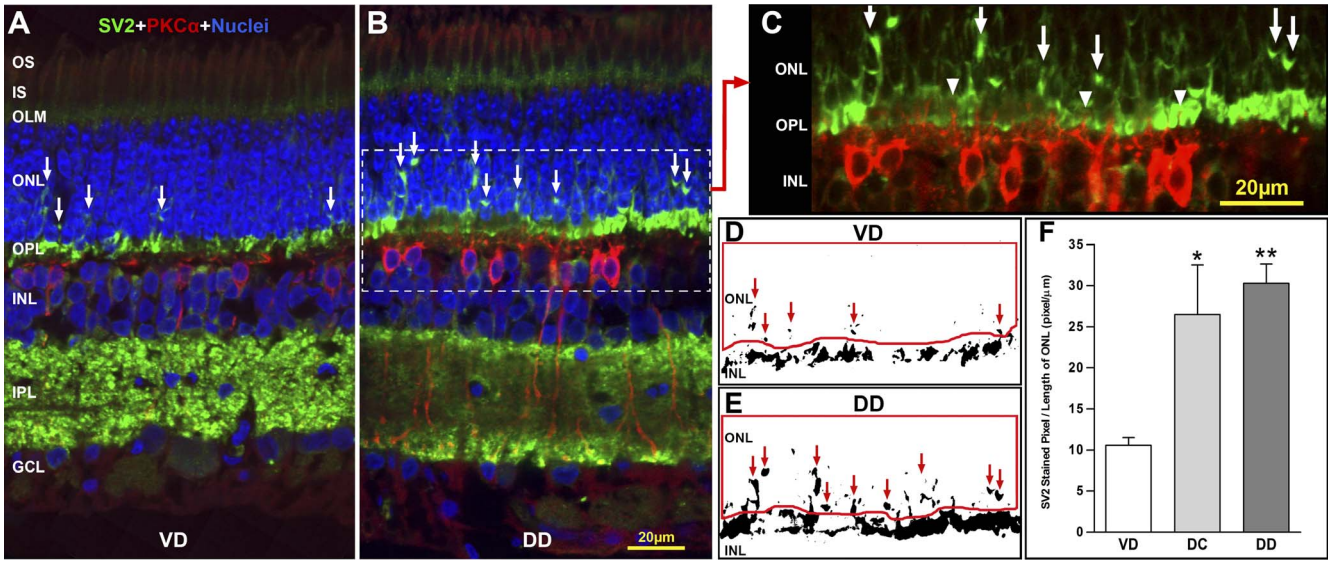

Figure 10. Quantification of axonal retraction 2 hours after retinal detachment in vivo. (**A**, **B**) Optical sections of 1 μm labeled for presynaptic terminals (SV2), bipolar cells (PKCα), and nuclei (PI). Retracted rod terminals in the ONL are shown (*arrows*). PKCα-labeled rod bipolar dendrites interact with rod spherules. DD, detached retina in operated eye; VD, area corresponding to the detached retina in the vitretomy-only eye. (**C**) Enlarged image of **B** (*dashed lines*). Immunolabeled bipolar dendrites do not extend beyond the OPL (*arrowheads*). (**D**, **E**) Binary images were created from **A** and **B**, respectively. The number of SV2-labeled pixels clustered in spots indicative of retracted spherules (*red arrows*) in the ONL, delimited by the *red border*, were determined and divided by the length of examined ONL. (**F**) More SV2-labeled pixels occurred in the retina with a detachment in both detached (DD) and attached (DC) areas than in retina from the eye that had undergone only vitrectomy (VD) ($^{*}P < 0.05$; $^{**}P < 0.01$; $n = 36$ retinal sections; three pigs).

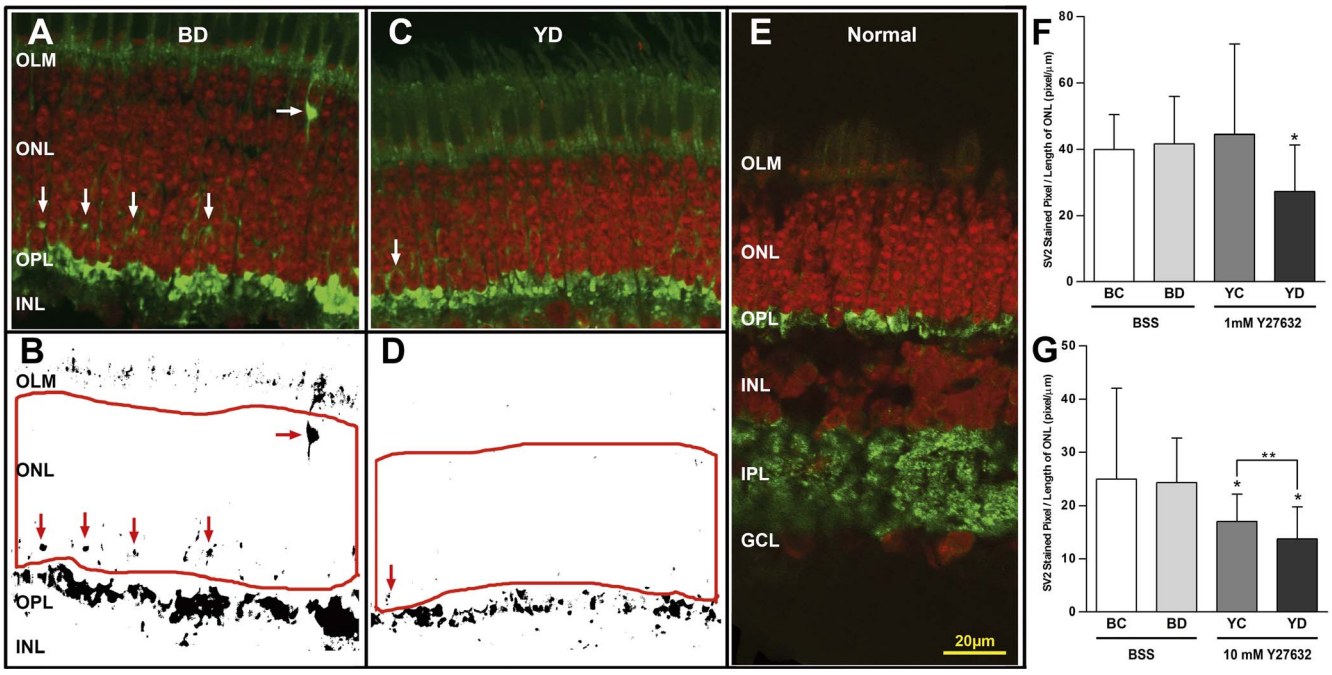

Figure 11. Effect of Y27632 on axonal retraction by photoreceptors after retinal detachment in vivo. (**A**, **C**) Representative confocal images of control detached retina (BD) and detached retina treated with 10 mM Y27632 (YD) labeled for SV2 (*green*) and nuclei (*red*). SV2-labeled spots (*white arrows*) in the ONL indicate axonal retraction. (**B**, **D**) Binary images created from **A**, **C**. SV2-labeled spots are indicated with *red arrows*. The number of labeled pixels in the ONL delimited by the *red borders* was determined and divided by the length of examined ONL as in Figure 10. (**E**) Normal retina without detachment is shown for comparison. (**F**, **G**) Treatment with 1 mM and 10 mM Y27632. Comparison of SV2-labeled pixels/unit retinal length in different retinal areas (BC and BD, attached and detached areas, respectively, in the eye using BSS for detachment; YC and YD, attached and detached areas, respectively, in the eye using Y27632 for detachment). In both treatment groups, there are no significant differences between BC and BD in SV2-labeled pixels. For 1 mM Y27632, labeled pixels in YD were 34.5% less than labeled pixels in BD ($^{*}P = 0.02$; $n = 48$ retinal sections; 16 samples; four pigs). There was also a reduction in pixel labeling to 38.7% in YD compared to that in YC ($P = 0.06$; $n = 48$ retinal sections; 16 samples; four pigs). For 10 mM Y27632, labeled pixels in YD and YC were 43.7% ($^{*}P = 0.02$) and 29.9% ($^{*}P = 0.04$), respectively, less than labeled pixels in BD. Thus, only with 10 mM Y27632 was there a reduction in pixel labeling in the YC area compared to that in BD. Finally, there was also a significant reduction in labeled pixels in YD compared to that in YC by 24.4% ($^{**}P = 0.009$; $n = 48$ retinal sections; 16 samples; four pigs).

Investigative Ophthalmology & Visual Science

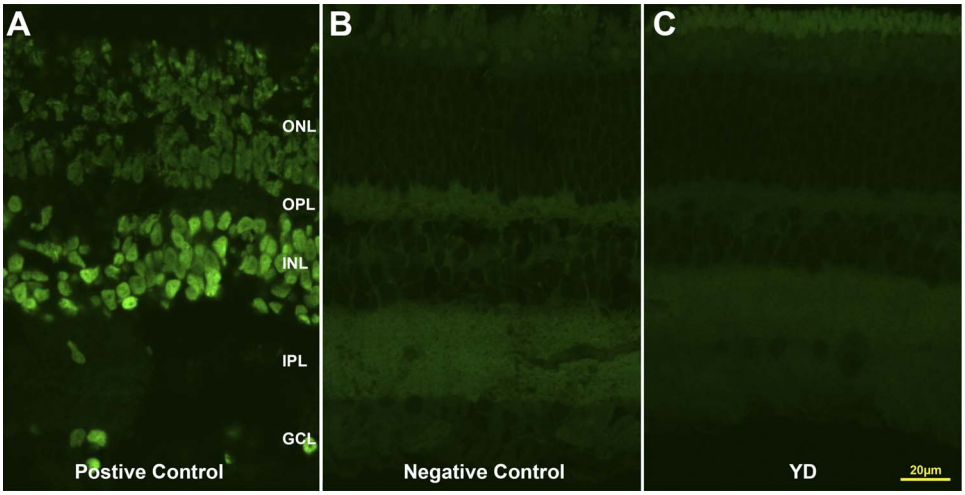

Figure 12. TUNEL staining of retina treated with 10 mM Y27632 in vivo. (**A**) Positive control using TACS nuclease. (**B**) Negative control, staining without using TdT enzyme. (**C**) No apoptotic cells were detected in the detached retina treated with 10 mM Y27632.

retraction spreads from the detached area to distant nondetached areas (Fig. 10). However, in both 1 mM and 10 mM Y27632-treated groups, the number of SV2-labeled pixels was lower in YD than in YC by 35.8% ($P = 0.06$) and 19.2% ($P = 0.004$), respectively, indicating that Y27632 is more effective at reducing retraction close to its injection site at the detachment compared to more distant, nondetached areas.

To examine whether Y27632 is toxic to the retina, sections from three animals treated with the highest dose of Y27632 (10 mM) were screened for cell death by looking for condensed and rounded nuclei stained by PI. Although a few pyknotic nuclei were found in the nontreated detached area (BD), especially in the ONL (1.3 cells per mm retina) and GCL (2.4 cells per mm of retina), virtually no cell death was found in the ONL, INL, or GCL in Y27632-treated detached area (YD). Labeling using the TUNEL technique revealed no positive staining for apoptotic cells (Fig. 12), suggesting Y27632 is not toxic to retinal cells at concentrations up to 10 mM. Additionally, the retinal layers of Y27632-treated but detached retina (Fig. 11C) appeared to be better organized and had less edema than untreated detached retina (Figs. 11A, 11B) and were comparable to normal retina (Fig. 11E). A reduction in pyknotic nuclei and preservation of retinal structure has been previously noted after treatment with RhoA-associated inhibitors.[45,46]

Discussion

Based on these results in the live pig, retina can be added to the list of CNS structures which show increased RhoA activity after injury. Activity was increased with detachment compared to both the untouched eyes and to the eyes which served as a control for surgical procedures and had a vitrectomy but no detachment. In addition, we have documented that significantly increased activity occurs very rapidly, within 2 hours after the insult. This observation is consistent with a previous qualitative observation that RhoA activity was increased 1.5 hours after a rat spinal cord injury.[4] Our current data from the in vitro model for detachment suggests that the beginning of the RhoA increase in the retina may be even earlier: in porcine retinal explants, significant increases were observed 10 minutes after injury (Fig. 3D). Early increases in activity may be the rule after CNS injury, but other than the retina and the spinal cord, this hypothesis has yet to be tested.

Increases in total RhoA protein were not observed after detachment in vivo. This result is supported by observations from the rat spinal cord injury model, where both RhoA mRNA and total protein levels showed no increase for many days after the injury,[3] even though activity was increased rapidly.[4] It is possible that increases in protein and RNA occurred later. The length of time over which high RhoA activity occurs is not yet known for retina. In patients, high RhoA protein levels have been observed months after focal cerebral infarction or traumatic brain injury[1,2] and 4 weeks after spinal cord injury in rats.[47] Finally, changes in Rho pathways in retina 2 hours after detachment were greater for RhoA signaling than for RAC1 activity, another Rho protein involved in cytoskeletal control. The relative values of RhoA and RAC1 signaling, however, may change over time (i.e., with longer detachments).

The retina, because of its layered structure, can be examined easily for changes in synaptic connectivity. First described in vivo in cat retina,[17] retraction of the rod axon and spherule after detachment has also been seen in human retina.[15,16] Our study demonstrates that retraction can occur by 2 hours. In porcine retina, the timing correlates well with increased RhoA activity. We also examined retinae for sprouting of bipolar dendrites, which has been described in other models,[18] at the 2-hour time point, and found no labeled processes in the ONL. We posit that dendritic rod bipolar sprouting occurs later. The lack of sprouting supports the electron microscopic findings that retraction leads to synaptic disjunction,[20] the spherule moves away as the dendrites stay in place. Our study suggests, therefore, that synaptic disjunction occurs by 2 hours. Whether the amount of disjunction results in reduced vision is presently unknown. However, visual field defects seen within the early days after detachment may be due not only to the separation of the photoreceptors from the RPE and thus reduced visual pigment regeneration and metabolic support for photoreceptors,[48,49] but also to reduced synaptic function.

A possible confounding factor in our studies was damage due to the surgery itself. In our procedure the vitreous was removed by a vitrectomy that included excision of the core vitreous as well as excision of the posterior hyaloid prior to detachment. Although low levels in RhoA activity and axonal retraction were seen after vitrectomy alone, dramatic increases were seen when both vitrectomy and detachment were performed. The increases in both RhoA activation and

Investigative Ophthalmology & Visual Science

retraction emphasize that the changes in activity and synaptic anatomy are related and indicate that the surgical procedures, other than detachment, such as the presence of epinephrine in the perfusate, were not the primary stimuli for RhoA activation. In the case of epinephrine, increased RhoA activity (shown here) and retraction[14] in retinal explants, where no epinephrine is used, demonstrate an absence of an effect by this compound on the RhoA pathway. We did find similar increases in GFAP and RAC1 with vitrectomy alone compared to vitrectomy and detachment. The increase in GFAP with vitrectomy alone but without large changes in synaptic retraction or RhoA activity suggests that changes in Müller cells are not the primary initiator of retraction and that GFAP can increase without an obvious increase in RhoA activity. ROCK inhibition can decrease GFAP levels when examined 7 days after optic nerve injury.[41] This report does not necessarily conflict with our results if RhoA activity primarily acts to sustain rather than initiate high GFAP levels. Our results are not in accordance, however, with those from a report in porcine retinal detachment which showed that GFAP was not increased by vitrectomy alone when observed 3 days after surgery.[40] The vitrectomy procedure in the previous report was limited, occurring only over the small area of a future detachment. Our data and this previous report suggest that GFAP increases in Müller cells are sensitive to mechanical perturbation in a graded fashion. Extensive vitrectomy (our procedure) may increase GFAP activity, but minor perturbations may not. A similar argument may be made for RAC1 activity. In our experiments, only RhoA activity dramatically increased with detachment compared to vitrectomy alone. Our surgical controls also emphasize that the ability to compare retinal detachment models will depend both upon surgical techniques (in addition to differing types of vitrectomy, some models include removal of the lens and insertion of sodium hyaluronate into the subretinal space for instance[19]), and the timing of the analysis (i.e., hours versus days after detachment).

A notable feature of our results was the presence of changes, increases in both RhoA activity and synaptic disjunction, in attached retina in the eyes with a detachment. Other injury responses have also been reported to spread within the retina. Decreased function,[50,51] gliosis,[40,52] photoreceptor degeneration,[53] and changes in the immune system[40] have all been reported in the attached portion of the retina from eyes with detachments. These reports come from a variety of mammalian models. In salamander retina, however, changes in glutamate and glutamine staining occurred only in the detached retina.[54] There may be interspecies differences; moreover, the salamander retina is avascular unlike most mammalian retinae. Although the cause(s) of the spread of retinal changes after injury is not known, the implications for therapy seem clear. It is not only the directly injured retina that suffers and must be protected. A similar situation occurs in spinal cord injury: both directly injured and more remote surrounding regions show increased RhoA-positive cells.[47] In our model, attached retina that was almost a centimeter away from the detached area was assessed, suggesting a fairly extensive spread of damage.

Although there are multiple known activators of RhoA activity, the mechanism(s) of RhoA activation in the injured retina is not yet known. However, we are beginning to understand how axonal retraction by rod photoreceptors occurs. Because ROCK inhibition and the blockage of L-type calcium channels reduce retraction in vitro, we had previously suggested that actomyosin contraction was important in axonal retraction (Fig. 1).[13,14,55] Here we tested whether MLC phosphorylation, necessary for contraction, increases in vivo in regions of retraction. There was indeed a significant increase in pMLC in detached retina. In the attached area, the increase, although present, did not reach statistical significance. This may be due to the small sample size and large variability. Alternatively, we now know that retraction depends not only on actomyosin contraction but also on actin filament turnover controlled by LIM kinase, which is in turn controlled by Rho pathways.[46] Thus, retraction could occur in attached retina by an alternative mechanism even if actomyosin contraction is weak. Finally, RAC1 may play some role in photoreceptor synaptic changes,[46] and its upregulation in detached retina may contribute to differences in regulation of retraction between the detached and attached areas.

Inhibition of ROCK using a subretinal injection of 1 or 10 mM of Y27632 at the inception of detachment in the pig was successful in reducing synaptic change in vivo. However, only at the highest dose was the drug successful in reducing synaptic change in nondetached regions of the retina. In vitro, lower doses of 1, 10, or 100 μM were sufficient to reduce axonal retraction.[14] Higher doses of Y27632 may be required in vivo because of reduced access and/or diffusion of the drug; in vitro, the isolated neural retina is immersed in the drug solution. Additionally, lack of a vascular circulation and uptake by the RPE may retain higher concentrations of drug in the ONL in vitro for longer periods of time. The final concentration of Y27632 in vivo is unknown. However, similar initial doses of ophthalmic drugs have been used in other applications: for example, a 0.4% solution (equivalent to 11 mM) of ripasudil hydrochloride hydrate, a small-molecule ROCK inhibitor, has been approved for the treatment of glaucoma and ocular hypertension.[56] Finally, although we cannot rule out nonspecific effects at higher doses, there was no apparent cytotoxicity after 2 hours of treatment.

In future studies, it will be critical to know how soon RhoA pathway inhibition is needed to preserve the retina after injury. For some types of human CNS injury, the time frame for intervention has become shorter and shorter. With stroke, for instance, the window in which to administer alteplase (a recombinant tissue plasminogen activator) has been reduced to within 3 hours after infarct for maximum benefit.[57] A similar shortening of time, to within 3 hours, has been suggested for treatment of acute spinal cord injury with antioxidant therapies.[58] Although the targets may differ for stroke and spinal cord injury, the idea of early intervention is well known to neurologists. For ophthalmologists, there has been debate about the role of timing of surgery in visual outcome among patients with macula-involving retinal detachment. The discussion has centered on whether visual outcome is substantially influenced by operating within 3 or 7 days or longer after the macula is detached.[59–69] At present, no studies of the duration of macula-involving rhegmatogenous detachment have been reported which include reattachment times in the hours after injury. Because our results indicate that synaptic damage has already occurred 2 hours after detachment, it may be worthwhile to reassess the optimal interval for intervention assessing subtle aspects of visual function (e.g., multifocal electroretinogram, microperimetry) in addition to best-corrected visual acuity.

Overall, the results for visual function after surgery for cases of macula-involving rhegmatogenous retinal detachment indicate that most operated eyes see significantly worse than the fellow eye.[59,70,71] Detachments that do not involve the macula have much better visual outcomes; however, visual recovery is still poor for approximately 25% of these patients.[62] The poor recovery might seem surprising as studies have shown that OS are restored after reattachment in animal models; in rhesus monkey, complete restoration was observed approximately 20 weeks after reattachment.[72] We and others[73] speculate that synaptic changes may stall visual recovery. In addition to axonal retraction, studies of animal models after reattachment

Investigative Ophthalmology & Visual Science

surgery demonstrate sprouting from rod terminals, with the new neurites reaching inappropriately into the inner retina.[74] Sprouting has also been described in human retinae with reattachment surgery.[15] These observations may mean that if rapid retinal reattachment surgery can preserve the original neural circuitry (an as-yet unproven hypothesis), rapid surgery may provide visual outcomes superior to those achieved with more delayed retinal reattachment procedures. Use of RhoA inhibitors might assist in further stabilizing the circuitry or might be used as an interim measure before reattachment surgery. RhoA inhibitors may also be useful in situations where displacement of retinal tissue is necessary for surgical implants, injection of viral vectors or trophic factors,[75–77] or in tissue transplantation.[78]

Acknowledgments

The authors thank Alcon (Fort Worth, TX, USA) for generous donation of the Accurus vitrectomy machine. The authors also thank Suresh Bhatt (veterinarian), Qian Sun, and Noounanong Cheewatrakoolpong for assistance in animal surgeries, Éva Halász for assistance in data analysis, and Amy Davidow for statistical advice.

Supported by US National Institutes of Health Grant EY021542.

Disclosure: **J. Wang**, None; **M. Zarbin**, None; **I. Sugino**, None; **I. Whitehead**, None; **E. Townes-Anderson**, None

References

1. Brabeck C, Beschorner R, Conrad S, et al. Lesional expression of RhoA and RhoB following traumatic brain injury in humans. *J Neurotrauma*. 2004;21:697–706.
2. Brabeck C, Mittelbronn M, Bekure K, Meyermann R, Schluesener HJ, Schwab JM. Effect of focal cerebral infarctions on lesional RhoA and RhoB expression. *Arch Neurol*. 2003;60:1245–1249.
3. Sung JK, Miao L, Calvert JW, Huang L, Louis Harkey H, Zhang JH. A possible role of RhoA/Rho-kinase in experimental spinal cord injury in rat. *Brain Res*. 2003;959:29–38.
4. Dubreuil CI, Winton MJ, McKerracher L. Rho activation patterns after spinal cord injury and the role of activated Rho in apoptosis in the central nervous system. *J Cell Biol*. 2003;162:233–243.
5. Dubreuil CI, Marklund N, Deschamps K, McIntosh TK, McKerracher L. Activation of Rho after traumatic brain injury and seizure in rats. *Exp Neurol*. 2006;198:361–369.
6. Petratos S, Li QX, George AJ, et al. The beta-amyloid protein of Alzheimer's disease increases neuronal CRMP-2 phosphorylation by a Rho-GTP mechanism. *Brain*. 2008;131:90–108.
7. Lehmann M, Fournier A, Selles-Navarro I, et al. Inactivation of Rho signaling pathway promotes CNS axon regeneration. *J Neurosci*. 1999;19:7537–7547.
8. Dergham P, Ellezam B, Essagian C, Avedissian H, Lubell WD, McKerracher L. Rho signaling pathway targeted to promote spinal cord repair. *J Neurosci*. 2002;22:6570–6577.
9. Yamashita K, Kotani Y, Nakajima Y, et al. Fasudil, a Rho kinase (ROCK) inhibitor, protects against ischemic neuronal damage in vitro and in vivo by acting directly on neurons. *Brain Res*. 2007;1154:215–224.
10. Hou Y, Zhou L, Yang QD, et al. Changes in hippocampal synapses and learning-memory abilities in a streptozotocin-treated rat model and intervention by using fasudil hydrochloride. *Neuroscience*. 2012;200:120–129.
11. Tonges L, Frank T, Tatenhorst L, et al. Inhibition of rho kinase enhances survival of dopaminergic neurons and attenuates axonal loss in a mouse model of Parkinson's disease. *Brain*. 2012;135:3355–3370.
12. Song Y, Chen X, Wang LY, Gao W, Zhu MJ. Rho kinase inhibitor fasudil protects against beta-amyloid-induced hippocampal neurodegeneration in rats. *CNS Neurosci Ther*. 2013;19:603–610.
13. Fontainhas AM, Townes-Anderson E. RhoA and its role in synaptic structural plasticity of isolated salamander photoreceptors. *Invest Ophthalmol Vis Sci*. 2008;49:4177–4187.
14. Fontainhas AM, Townes-Anderson E. RhoA inactivation prevents photoreceptor axon retraction in an in vitro model of acute retinal detachment. *Invest Ophth Vis Sci*. 2011;52:579–587.
15. Fisher SK, Lewis GP. Müller cell and neuronal remodeling in retinal detachment and reattachment and their potential consequences for visual recovery: a review and reconsideration of recent data. *Vision Res*. 2003;43:887–897.
16. Sethi CS, Lewis GP, Fisher SK, et al. Glial remodeling and neural plasticity in human retinal detachment with proliferative vitreoretinopathy. *Invest Ophth Vis Sci*. 2005;46:329–342.
17. Erickson PA, Fisher SK, Anderson DH, Stern WH, Borgula GA. Retinal detachment in the cat: the outer nuclear and outer plexiform layers. *Invest Ophthalmol Vis Sci*. 1983;24:927–942.
18. Lewis GP, Linberg KA, Fisher SK. Neurite outgrowth from bipolar and horizontal cells after experimental retinal detachment. *Invest Ophthalmol Vis Sci*. 1998;39:424–434.
19. Lewis GP, Matsumoto B, Fisher SK. Changes in the organization and expression of cytoskeletal proteins during retinal degeneration induced by retinal detachment. *Invest Ophthalmol Vis Sci*. 1995;36:2404–2416.
20. Linberg KA, Lewis GP, Fisher SK. Retraction and remodeling of rod spherules are early events following experimental retinal detachment: an ultrastructural study using serial sections. *Mol Vis*. 2009;15:10–25.
21. Prince JH, Ruskell GL. The use of domestic animals for experimental ophthalmology. *Am J Ophthalmol*. 1960;49:1202–1207.
22. Simoens P, De Schaepdrijver L, Lauwers H. Morphologic and clinical study of the retinal circulation in the miniature pig. A: morphology of the retinal microvasculature. *Exp Eye Res*. 1992;54:965–973.
23. Gerke C, Hao Y, Wong F. Topography of rods and cones in the retina of the domestic pig. *Hong Kong Med J*. 1995;1:302–308.
24. Wang J, Kolomeyer AM, Zarbin MA, Townes-Anderson E. Organotypic culture of full-thickness adult porcine retina. *J Vis Exp*. 2011;pii:2655. Available at: http://www.jove.com/Details.php?ID=2655.
25. Glaven JA, Whitehead I, Bagrodia S, Kay R, Cerione RA. The Dbl-related protein, Lfc, localizes to microtubules and mediates the activation of Rac signaling pathways in cells. *J Biol Chem*. 1999;274:2279–2285.
26. Degasperi A, Birtwistle MR, Volinsky N, Rauch J, Kolch W, Kholodenko BN. Evaluating strategies to normalise biological replicates of Western blot data. *PLoS One*. 2014;9:e87293.
27. Aoki J, Taira A, Takanezawa Y, et al. Serum lysophosphatidic acid is produced through diverse phospholipase pathways. *J Biol Chem*. 2002;277:48737–48744.
28. Sayas CL, Moreno-Flores MT, Avila J, Wandosell F. The neurite retraction induced by lysophosphatidic acid increases Alzheimer's disease-like Tau phosphorylation. *J Biol Chem*. 1999;274:37046–37052.
29. Brewer GJ, Torricelli JR, Evege EK, Price PJ. Optimized survival of hippocampal neurons in B27-supplemented Neurobasal, a

new serum-free medium combination. *J Neurosci Res*. 1993; 35:567–576.

30. Santos-Bredariol AS, Santos MF, Hamassaki-Britto DE. Distribution of the small molecular weight GTP-binding proteins Rac1, Cdc42, RhoA and RhoB in the developing chick retina. *J Neurocytol*. 2002;31:149–159.
31. Auer M, Hausott B, Klimaschewski L. Rho GTPases as regulators of morphological neuroplasticity. *Ann Anat*. 2011; 193:259–266.
32. Albertinazzi C, Gilardelli D, Paris S, Longhi R, de Curtis I. Overexpression of a neural-specific rho family GTPase, cRac1B, selectively induces enhanced neuritogenesis and neurite branching in primary neurons. *J Cell Biol*. 1998;142: 815–825.
33. Chan D, Citro A, Cordy JM, Shen GC, Wolozin B. Rac1 protein rescues neurite retraction caused by G2019S leucine-rich repeat kinase 2 (LRRK2). *J Biol Chem*. 2011;286:16140–16149.
34. Ren XD, Wang R, Li Q, Kahek LA, Kaibuchi K, Clark RA. Disruption of Rho signal transduction upon cell detachment. *J Cell Sci*. 2004;117:3511–3518.
35. Gallo G. Myosin II activity is required for severing-induced axon retraction in vitro. *Exp Neurol*. 2004;189:112–121.
36. Lin-Jones J, Sohlberg L, Dose A, Breckler J, Hillman DW, Burnside B. Identification and localization of myosin superfamily members in fish retina and retinal pigmented epithelium. *J Comp Neurol*. 2009;513:209–223.
37. Joo EE, Yamada KM. MYPT1 regulates contractility and microtubule acetylation to modulate integrin adhesions and matrix assembly. *Nat Communs*. 2014;5:3510.
38. Murthy KS, Zhou H, Grider JR, Brautigan DL, Eto M, Makhlouf GM. Differential signalling by muscarinic receptors in smooth muscle: m2-mediated inactivation of myosin light chain kinase via Gi3, Cdc42/Rac1 and p21-activated kinase 1 pathway, and m3-mediated MLC20 (20 kDa regulatory light chain of myosin II) phosphorylation via Rho-associated kinase/myosin phosphatase targeting subunit 1 and protein kinase C/CPI-17 pathway. *Biochem J*. 2003;374:145–155.
39. Ryan SJ. *Retina*. 4th ed. Philadelphia: Elsevier/Mosby; 2006.
40. Iandiev I, Uckermann O, Pannicke T, et al. Glial cell reactivity in a porcine model of retinal detachment. *Invest Ophthalmol Vis Sci*. 2006;47:2161–2171.
41. Tura A, Schuettauf F, Monnier PP, Bartz-Schmidt KU, Henke-Fahle S. Efficacy of Rho-kinase inhibition in promoting cell survival and reducing reactive gliosis in the rodent retina. *Invest Ophthalmol Vis Sci*. 2009;50:452–461.
42. Khodair MA, Zarbin MA, Townes-Anderson E. Synaptic plasticity in mammalian photoreceptors prepared as sheets for retinal transplantation. *Invest Ophthalmol Vis Sci*. 2003; 44:4976–4988.
43. Uehata M, Ishizaki T, Satoh H, et al. Calcium sensitization of smooth muscle mediated by a Rho-associated protein kinase in hypertension. *Nature*. 1997;389:990–994.
44. Zhang JY, Dong HS, Oqani RK, Lin T, Kang JW, Jin DI. Distinct roles of ROCK1 and ROCK2 during development of porcine preimplantation embryos. *Reproduction*. 2014;148:99–107.
45. Kita T, Hata Y, Arita R, et al. Role of TGF-beta in proliferative vitreoretinal diseases and ROCK as a therapeutic target. *Proc Natl Acad Sci U S A*. 2008;105:17504–17509.
46. Wang W, Townes-Anderson E. LIM kinase, a newly identified regulator of presynaptic remodeling by rod photoreceptors after injury. *Invest Ophthalmol Vis Sci*. 2015;56:7847–7858.
47. Conrad S, Schluesener HJ, Trautmann K, Joannin N, Meyermann R, Schwab JM. Prolonged lesional expression of RhoA and RhoB following spinal cord injury. *J Comp Neurol*. 2005; 487:166–175.
48. Steinberg RH. Research update: report from a workshop on cell biology of retinal detachment. *Exp Eye Res*. 1986;43:695–706.
49. Mervin K, Valter K, Maslim J, Lewis G, Fisher S, Stone J. Limiting photoreceptor death and deconstruction during experimental retinal detachment: the value of oxygen supplementation. *Am J Ophthalmol*. 1999;128:155–164.
50. Chisholm IA, McClure E, Foulds WS. Functional recovery of the retina after retinal detachment. *Trans Ophthalmol Soc U K*. 1975;95:167–172.
51. Sasoh M, Yoshida S, Kuze M, Uji Y. The multifocal electroretinogram in retinal detachment. *Doc Ophthalmol*. 1997;94: 239–252.
52. Francke M, Faude F, Pannicke T, et al. Electrophysiology of rabbit Müller (glial) cells in experimental retinal detachment and PVR. *Invest Ophthalmol Vis Sci*. 2001;42:1072–1079.
53. Faure J, Dagher MC. Interactions between Rho GTPases and Rho GDP dissociation inhibitor (Rho-GDI). *Biochimie*. 2001; 83:409–414.
54. Sherry DM, Townes-Anderson E. Rapid glutamatergic alterations in the neural retina induced by retinal detachment. *Invest Ophthalmol Vis Sci*. 2000;41:2779–2790.
55. Nachman-Clewner M, Townes-Anderson E. Injury-induced remodelling and regeneration of the ribbon presynaptic terminal in vitro. *J Neurocytol*. 1996;25:597–613.
56. Garnock-Jones KP. Ripasudil: first global approval. *Drugs*. 2014;74:2211–2215.
57. Emberson J, Lees KR, Lyden P, et al. Effect of treatment delay, age, and stroke severity on the effects of intravenous thrombolysis with alteplase for acute ischaemic stroke: a meta-analysis of individual patient data from randomised trials. *Lancet*. 2014;384:1929–1935.
58. Hall ED. Antioxidant therapies for acute spinal cord injury. *Neurotherapeutics*. 2011;8:152–167.
59. Burton TC. Recovery of visual acuity after retinal detachment involving the macula. *Trans Am Ophthalmol Soc*. 1982;80: 475–497.
60. Ross WH, Kozy DW. Visual recovery in macula-off rhegmatogenous retinal detachments. *Ophthalmology*. 1998;105:2149–2153.
61. Tani P, Robertson DM, Langworthy A. Prognosis for central vision and anatomic reattachment in rhegmatogenous retinal detachment with macula detached. *Am J Ophthalmol*. 1981; 92:611–620.
62. Salicone A, Smiddy WE, Venkatraman A, Feuer W. Visual recovery after scleral buckling procedure for retinal detachment. *Ophthalmology*. 2006;113:1734–1742.
63. Girard P, Karpouzas I. Visual acuity after scleral buckling surgery. *Ophthalmologica*. 1995;209:323–328.
64. Liu F, Meyer CH, Mennel S, Hoerle S, Kroll P. Visual recovery after scleral buckling surgery in macula-off rhegmatogenous retinal detachment. *Ophthalmologica*. 2006;220:174–180.
65. Diederen RM, La Heij EC, Kessels AG, Goezinne F, Liem AT, Hendrikse F. Scleral buckling surgery after macula-off retinal detachment: worse visual outcome after more than 6 days. *Ophthalmology*. 2007;114:705–709.
66. Henrich PB, Priglinger S, Klaessen D, et al. Macula-off retinal detachment–a matter of time? *Klin Monbl Augenheilkd*. 2009; 226:289–293.
67. Mowatt L, Shun-Shin GA, Arora S, Price N. Macula off retinal detachments. How long can they wait before it is too late? *Eur J Ophthalmol*. 2005;15:109–117.
68. Ross W, Lavina A, Russell M, Maberley D. The correlation between height of macular detachment and visual outcome in

macula-off retinal detachments of < or = 7 days' duration. *Ophthalmology*. 2005;112:1213–1217.

69. van Bussel EM, van der Valk R, Bijlsma WR, La Heij EC. Impact of duration of macula-off retinal detachment on visual outcome: a systematic review and meta-analysis of literature. *Retina*. 2014;34:1917–1925.
70. Ross WH, Stockl FA. Visual recovery after retinal detachment. *Curr Opin Ophthalmol*. 2000;11:191–194.
71. Ozgur S, Esgin H. Macular function of successfully repaired macula-off retinal detachments. *Retina*. 2007;27:358–364.
72. Guerin CJ, Lewis GP, Fisher SK, Anderson DH. Recovery of photoreceptor outer segment length and analysis of membrane assembly rates in regenerating primate photoreceptor outer segments. *Invest Ophthalmol Vis Sci*. 1993;34:175–183.
73. Lewis GP, Charteris DG, Sethi CS, Fisher SK. Animal models of retinal detachment and reattachment: identifying cellular events that may affect visual recovery. *Eye (Lond)*. 2002;16:375–387.
74. Lewis GP, Sethi CS, Linberg KA, Charteris DG, Fisher SK. Experimental retinal reattachment: a new perspective. *Mol Neurobiol*. 2003;28:159–175.
75. Bainbridge JW, Smith AJ, Barker SS, et al. Effect of gene therapy on visual function in Leber's congenital amaurosis. *N Engl J Med*. 2008;358:2231–2239.
76. Maguire AM, Simonelli F, Pierce EA, et al. Safety and efficacy of gene transfer for Leber's congenital amaurosis. *N Engl J Med*. 2008;358:2240–2248.
77. Hauswirth WW, Aleman TS, Kaushal S, et al. Treatment of leber congenital amaurosis due to RPE65 mutations by ocular subretinal injection of adeno-associated virus gene vector: short-term results of a phase I trial. *Hum Gene Ther*. 2008;19:979–990.
78. Schwartz SD, Regillo CD, Lam BL, et al. Human embryonic stem cell-derived retinal pigment epithelium in patients with age-related macular degeneration and Stargardt's macular dystrophy: follow-up of two open-label phase 1/2 studies. *Lancet*. 2015;385:509–516.

Investigative Ophthalmology & Visual Science